Chemical Engineering Journal 165 (2010) 17–25

Contents lists available at ScienceDirect

Chemical Engineering Journal

journal homepage: www.elsevier.com/locate/cej

# Iron and chromium sulfates from ferrochromium alloy for tanning

Bruno München Wenzel[a,*], Nilson Romeu Marcilio[a], Marcelo Godinho[b], Leonardo Masotti[a], Celso Brisolara Martins[a]

[a] Laboratory of Wastes Treatment (LPR), Chemical Engineering Department, Federal University of Rio Grande do Sul, Luiz Englert str., s/n, 90040-040 Porto Alegre, RS, Brazil
[b] Chemical Engineering Department, University of Caxias do Sul, Francisco Getúlio Vargas str.,130, 95070-560 Caxias do Sul, RS, Brazil

ARTICLE INFO

*Article history:*
Received 10 May 2010
Received in revised form 10 August 2010
Accepted 17 August 2010

*Keywords:*
Tanning agent
Ferrochromium alloy
Box–Behnken design
Iron and chromium sulfate

ABSTRACT

In this study we investigated the production of soluble iron and chromium sulfate complexes from high carbon ferrochromium alloy (Fe–Cr–HC) for utilization as a tanning agent. The temperature, sulfuric acid concentration, and the reaction time between Fe–Cr–HC and sulfuric acid were selected as independent variables for iron and chromium conversion. A quadratic response surface model was adjusted using the Box–Behnken statistical experimental design technique. The results obtained by solving multi-objective optimization problem have shown about 98.6–100% Cr and 86.9–89.1% Fe conversions. Perchloric acid and ammonium sulfate additions were investigated in order to determine the system limitations. The results have showed that an increase of perchloric acid concentration decreased the quantity of soluble chromium and iron compounds, while an ammonium sulfate addition improved the conversion of chromium up to 100%.



## 1. Introduction

Basic chromium sulfate (trivalent) is the most utilized tanning agent for hide stabilization against microbial degradation. Its application provides great versatility of the leather, excellent chemical properties and hydrothermal stability among others. However, chromium is considered to be very harmful for living cells, and may cause cancer [1,2] and cell death [3]. Chromium(III) species are potentially dangerous because can be metabolized in the living organisms to more toxic hexavalent form [2,4].

During the tanning process, huge amount of wastewaters, sludge and solid residues containing chromium(III) is produced [5,6]. In specific environmental conditions chromium(III) can be converted to chromium(VI) [7,8]. During normal tanning operation, the exhaustion of chromium is between 40% and 70% only. It means that the development of chromium high exhaustion systems and methods for its recovery and reuse [9,10] is an important environmental issue for minimization of wastewater and sludge pollution. A thermal treatment of solid wastes has been successfully applied [11,12] where chromium was recovered from ash [13–15].

A possible solution for chromium pollution from tannery wastes is to develop new tanning agents (mineral and organic) producing leathers with similar to the wet blue properties. This alternative has also been a subject of several studies (see the review of Sreeram and Ramasami [9]).

Applying the principal of analogy from iron–protein combination in the nature, iron has been considered as an effective mineral-tanning agent [16,17]. Iron is less toxic than chromium and when used with natural materials (as vegetable tannins) acting like mordant, generates natural colors, which could substitute for the synthetic azo dyes [18,19]. Azo dyes represent the most of dye market [19] despite of being a serious hazard for the environment and human health [20]. Iron-tetrakis (hydroxymethyl) phosphonium (THP) complex has also been proven to be an effective tanning agent [21]. Fathima et al. [22] reported the use of Fe–THP complex for stabilization of type I collagen and achievement of shrinkage and denaturation at 95 °C. The enzymatic stability of Fe–THP treated collagen was reported to be 2% during 72 h of incubation time and given operational conditions such as: 20:1 collagen:enzyme ratio at 37 °C [22].

Tavani and Lacour [23] investigated the production of iron(III) tanning salt from iron(III) sulfate heptahydrate from the waste of a titanium recovery process. The authors utilized cream of tartar ($C_4H_5O_6K$) to form soluble complexes with iron(III). The production of this salt with a good quality is achieved by applying spray drying (rapid drying) downstream process at low temperature. The quality was controlled by a residual hydration of salt for prolonged period of time and formation of iron(II) compounds [23]. A strategy to avoid unsuitable stability is based on an immediate utilization of salts during the tanning process. Tavani and

* Corresponding author. Tel.: +55 51 3308 3956; fax: +55 51 3308 3277.
*E-mail addresses:* bruno@enq.ufrgs.br (B.M. Wenzel), nilson@enq.ufrgs.br (N.R. Marcilio).

1385-8947/$ – see front matter © 2010 Elsevier B.V. All rights reserved.
doi:10.1016/j.cej.2010.08.047

**Table 1**
Composition of Fe–Cr–HC alloy used in the experiments (wt%).

| Cr | Fe[a] | C | Si | Ti | P | S |
|---|---|---|---|---|---|---|
| 52.4 | 36.2 | 7.4 | 3.7 | 0.23 | 0.028 | 0.028 |

[a] By difference.

Lacour [23] obtained wet brown leather at shrinking temperature of 86 °C.

Due to the inherent disadvantages of the process when only iron salts were used (because of the iron salt stability), a partial replacement of chromium (i.e. less-chrome process) in tanning industry was developed. Rao et al. [24] proposed a process for preparation of chromium–iron complex which was used in leather industry. This process involves the following steps: (1) mixing the iron salt with chromium(VI) in water, addition of sulfuric acid, reducing agent and organic ligand (operational conditions: temperature range from 85 to 105 °C; process time 8–12 h; pH in the range from 2.5 to 2.8). (2) Second step includes conventional drying.

The properties of chromium–iron complexes-treated skins were reported by different authors as follows: shrinkage temperature = 115 °C [19], or 110 °C [17]; exhaustion bath for chromium = 92% [17] or 94% [17]; and 91% for iron [19]; spent tan liquor = 300 ppm Cr and 260 ppm Fe [19], 876 ppm Cr [17]. For the other physical-chemical characteristics, no significant differences were observed. This result seems to be very promising when compared with the one obtain with basic chromium sulfate (BCS) and iron salts (IS): shrinkage temperature = BCS 113 °C [17], BCS 116 °C [25], BCS–THP 109 °C [26], IS–THP 95 °C [22], IS 86 °C [23], IS 75 °C (cited by [19]); exhaustion bath = BCS 65% for chromium [25], BCS–THP 89% for chromium [26], 35% for iron (cited by [19]); spent tan liquor = 3000 ppm Cr [25], and 14,000 ppm Fe (cited by [19]).

In this work we developed a method for production of soluble iron and chromium sulfate complex from high carbon ferrochromium alloy (Fe–Cr–HC). The utilization of Fe–Cr–HC for production of tanning agent has advantage to avoid the step of formation of hexavalent chromium in the management cycle. The reaction was studied through a Box–Behnken experimental design [27,28] for the following independent variables: temperature of the process, sulfuric acid concentration and reaction time. A quadratic response surface model for conversion of iron and chromium was obtained.

For verification of the reaction limiting conditions, the additions of perchloric acid and ammonium sulfate were studied. These compounds were chosen because they have different influence on the reaction system behavior. The action of perchloric acid is connected to the breakage of the links between alloy atoms [29], while the ammonium sulfate increases the solubility of reaction products [30].

## 2. Experimental set-up

### 2.1. Materials and experimental procedure

The experiments were performed with commercial high carbon ferrochromium alloy (Fe–Cr–HC). The composition of Fe–Cr–HC used in the lixiviation experiments is shown in Table 1. Other reagents used in experiments were: solutions of sulfuric acid, perchloric acid (assay 70%) and ammonium sulfate ($(NH_4)_2SO_4$) with 99% purity.

The experimental apparatus (leaching equipment) consisted of a glass vessel (1 L) placed in a hot plate with magnetic stirrer. The vessel included 3 ports: for the thermometer, the condenser (cooled with water) and the sample placement. The condenser was used to keep constant concentration of acid solution by condensing the water vapor back to the reactor vessel.

**Table 2**
Values of the three levels of the independent variables (factors) investigated in linearly-deformed Box–Benhken design.

| Factor | Level | | |
|---|---|---|---|
| | −1 | 0 | +1 |
| $t$ (h) | 1 | 2 | 3 |
| $C$ (wt%) | 60 | | |
| $T$ (°C) | 110 | 130 | 150 |
| $C$ (wt%) | | 75 | |
| $T$ (°C) | 130 | 150 | 170 |
| $C$ (wt%) | | | 90 |
| $T$ (°C) | 150 | 170 | 190 |

Ferrochromium alloy (5 g) with 62 μm size (pass of sieve 250 mesh Tyler) was used. During the experiments, the initial solid/liquid ratio was kept 1/25 g of Fe–Cr–HC/ml $H_2SO_4$ solution. A high agitation velocity was maintained during the process time in order to ensure good mixing.

The experimental procedure was as follows: 125 ml of sulfuric acid solution (and perchloric acid, when used) were placed in a glass vessel with control heating. When the solution reached the desired temperature, 5 g of Fe–Cr–HC and $(NH_4)_2SO_4$ (when used) were added into the vessel and the start of the process time was set-up. At the end of the pre-established reaction time, the heating was turned off and the glass vessel was cooled down. The obtained solution was diluted and filtered using filter paper (25 μm medium size of pores). The filter residue was washed with hot distilled water and the total solution was diluted to a desired volume. Samples taken from the final solution were analyzed to quantify the Cr and Fe using graphite furnace atomic absorption spectrometry (GF-AAS).

The response variables were the conversion of iron and chromium from the Fe–Cr–HC alloy to soluble iron and chromium sulfates ($X_{Fe}$ and $X_{Cr}$, respectively).

### 2.2. Box–Behnken surface response design

Initially, the reaction between Fe–Cr–HC alloy and sulfuric acid was studied in three-variable Box–Behnken experimental design described by Dean and Voss [31]. This experimental project was deformed linearly in the concentration–temperature plane space and was adopted to run the process at atmospheric pressure conditions. The investigated variables in this part were: $H_2SO_4$ mass concentration in leaching solution ($C$), temperature ($T$) and reaction time ($t$).

To predict the responses ($X_{Cr}$ and $X_{Fe}$) of the experimental Box–Behnken design, a quadratic response surface model (see Eq. (1)) was proposed. In Table 2, the chosen three levels of variables $C$, $T$ and $t$ are shown.

$$X_i^{mod} = b_0^i + b_1^i C_C + b_2^i T_C + b_3^i t_C + b_{12}^i C_C T_C + b_{13}^i C_C t_C + b_{23}^i T_C t_C + b_{11}^i C_C^2 + b_{22}^i T_C^2 + b_{33}^i t_C^2 \quad (1)$$

where: $X_i^{mod}$ is the predicted conversion (%) of "$i$th" specie ($i$ = Cr, Fe) in Fe–Cr–HC for soluble sulfate compounds; $b_j^i$ ($j$ = 0, 1, 2, 3) is the parameter of linear effect of "$j$th" factor; $b_{kl}^i$ ($k$ and $l$ = 1, 2, 3; $kl = lk$) is the quadratic effect parameter of "$k$th" factor when $k$ = l, and the interaction effect parameter of "$k$th" and "lst" factor of model when $k \neq$ l; $C_C$, $T_C$ and $t_C$ are the coded factors (independent variables) of the model, represented by Eqs. (2), (3) and (4), respectively.

$$C_C = \frac{C - C_0}{\Delta C} \quad (2)$$

$$T_C = \frac{T - T_0}{\Delta T} - \frac{C - C_0}{\Delta C} \quad (3)$$

$$t_C = \frac{t - t_0}{\Delta t} \quad (4)$$

where: $C_0 = 75$ wt%, $T_0 = 150\,^{\circ}C$ and $t_0 = 2$ h is the central point of experimental region; $\Delta C = 15$ wt%, $\Delta T = 20\,^{\circ}C$ and $\Delta t = 1$ h are the intervals between levels of variables.

The total number of experiments required for surface response of three-variables Box–Behnken design was 15, including triplicate at the central point.

The model parameters were estimated by applying the general solution.

### 2.3. Statistical analysis

For evaluation of the predictive power of the proposed models, the coefficient of determination ($R^2$) and the adjusted coefficient of determination ($R^2_{adjusted}$) were calculated (Eqs. (5) and (6), respectively).

$$R^2 = 1 - \frac{RSS_{mod}}{SS_{exp}} = 1 - \frac{\sum_{i=1}^{n}(X_i^{mod} - X_i^{exp})^2}{\sum_{i=1}^{n}(X_i^{exp} - \overline{X}_{exp})^2} \quad (5)$$

$$R^2_{adjusted} = 1 - \left(\frac{n-1}{n-np}\right)\frac{RSS_{mod}}{SS_{exp}} \quad (6)$$

where: $RSS_{mod}$ is the residual sum square of the model; $SS_{exp}$ is the total sum of squares; $n$ is the number of performed experiments; $X_i^{mod}$ is the predicted value of conversion for "$i$th" experiment; $X_i^{exp}$ is the experimental value of conversion for "$i$th" experiment; $\overline{X}_{exp}$ is the mean of experimental results; np is the number of model parameters.

To verify the adequacy of the models we applied the $F$-test, comparing a variance associated with the model (between groups) with a variance associated with the experimental data (within the group). The null hypothesis assumes that the model variance is comparable to the experimental variance, so the model will be adequate. The value of $F$ for comparison with the critical (tabulated) value is given by Eq. (7).

$$F_0 = \frac{Var_{mod}}{Var_{exp}} = \frac{RSS_{mod}}{n-np} \Big/ \frac{RSS_{exp}}{nr(r-1)} \quad (7)$$

where: $Var_{mod}$ is the variance of the model; $Var_{exp}$ is the experimental variance (considered constant and determined at the central point of experimental region); $RSS_{exp}$ is the sum of square residuals associated with the experimental data (see Eq. (8)); nr = 1 is the number of points that replicated the experiments; $r = 3$ is the number of repetitions.

$$RSS_{exp} = \sum_{k=1}^{nr}\left[\sum_{j=1}^{r}(X_{k,j}^{exp} - \overline{X}_k^{exp})^2\right] \quad (8)$$

In Eq. (8): $X_{k,j}^{exp}$ is the experimental value of conversion at "$k$th" point, where repetitions occurs; $\overline{X}_k^{exp}$ is the mean of repetitions at "$k$th" experimental point.

The $t$-test was utilized to determine how significantly the parameter was different from zero (note—the null hypothesis considers the parameter values zero). The variance associated with the parameter is represented by the main diagonal of the parameter covariance matrix. Thus, some parameters were discharged from the model after analyzing the covariance matrix.

For models' comparison (initial model and the model with discharged parameters), the $F$-test was applied. The obtained value of $F$ for comparison with the critical (tabulated) value is given by Eq. (9). The null hypothesis assumes that a variance associated with the generic models "B" and "A" (variability between groups), is comparable to the variance associated with the model "B" (variability within the group). Model "B" includes more parameters than the model "A". Hence, if the null hypothesis is true, the model "B" will not be more adequate than the model "A".

$$F_0 = \frac{Var_{modA-B}}{Var_{modB}} = \left(\frac{RSS_A - RSS_B}{np_B - np_A}\right) \Big/ \left(\frac{RSS_B}{n - np_B}\right) \quad (9)$$

where: $RSS_k$ is the residual sum square of model "$k$"; $np_k$ is the number of parameters of model "$k$".

By adapting this methodology to our case, we were able to compare the models' quality—before and after the application of parameter significance test.

**Table 3**
Control experiments with/without perchloric acid addition ($t = 2$ h and $C = 75$ wt%).

| Run | $T$ (°C) | $R_{PA}$[a] |
|---|---|---|
| PA1 | 170 | 0 |
| PA2 | 170 | 1/4 |
| PA3 | 170 | 1/2 |
| PA4 | 140 | 0 |
| PA5 | 140 | 1/4 |
| PA6 | 140 | 1/2 |

[a] ml of $HClO_4$ 70%/g of Fe–Cr–C alloy.

### 2.4. Process optimization

For maximization of chromium and iron conversion, the multi-objective optimization problem has been transformed to scalar optimization problem by weighted sum method. The resulting objective function is given by Eq. (10).

$$F_{obj} = w_{Cr}X_{Cr}^{mod} + (1 - w_{Cr})X_{Fe}^{mod} \quad (10)$$

where: $F_{obj}$ is the objective function value; $w_{Cr}$ is the "weight" adopted for chromium conversion.

The trust-region-reflective algorithm (a subspace trust-region method based on the interior-reflective Newton method) described in [32] was used for maximization of the objective function.

### 2.5. Effect of perchloric acid and ammonium sulfate addition

During the independent set of experiments, the effect of addition of ammonium sulfate ($(NH_4)_2SO_4$) ($R_{AS}$) and perchloric acid ($HClO_4$) ($R_{PA}$) into the reaction system was studied. $HClO_4$ was utilized to improve the reaction rate due to its high oxidative potential and high acid power [29,33]. In other hand, $(NH_4)_2SO_4$ was used to increase the solubility of chromium and iron sulfates [30,34]. The investigation of these variables helped to determine the process limitation: more particularly in what extend $H_2SO_4$ solution oxidized chromium and iron, and how much of them precipitated as anhydrous iron(II) or chromium(III) sulfate (verified by [29]), or in what range of concentrations the oxidative potential of this acid solution was insufficient to complete the reaction.

The quantities of $HClO_4$ utilized during the experiments were represented by $R_{PA}$ ratio. More particularly, they were defined by the ratio of $HClO_4$ and Fe–Cr–HC. Additional six control experiments were performed. Two of them were designed without addition of $HClO_4$, and the other four were executed with different ratios such as—0.25 and 0.5 ml of $HClO_4$ 70%/g of Fe–Cr–HC (see Table 3). The operational conditions were as follows: $t = 2$ h, $C = 75$ wt%; and the process temperatures were set-up at two levels 140 °C and 170 °C.

The $(NH_4)_2SO_4$ quantities were represented by $R_{AS}$. The $R_{AS}$ ratio was determined taking into account the stoichiometry of formation of ammonium chrome alum ($NH_4Cr(SO_4)_2{\cdot}12H_2O$) according to the

**Table 4**
Experiments with/without ammonium sulfate addition ($t$ = 2h).

| Run | $T$ (°C) | $C$ (wt%) | $R_{AS}$[a] |
|---|---|---|---|
| 10 | 150 | 60 | −100.0 |
| AS1 | 150 | 60 | 0 |
| AS2 | 150 | 60 | 80.4 |
| AS3 | 150 | 60 | 170.6 |
| AS4 | 170 | 75 | −100.0 |
| AS5 | 170 | 75 | 0 |
| AS6 | 170 | 75 | 80.4 |
| AS7 | 170 | 75 | 170.6 |

[a] % of excess of ammonium sulfate in relation to the stoichiometric amount.

non-equilibrium reaction (see Eq. (11)). Hence, the calculated stoichiometric amount of $R_{AS}$ was equal to 0.6651 g $(NH_4)_2SO_4$ per g Fe–Cr–HC.

$$2Cr + 3H_2SO_4 + (NH_4)_2SO_4 \xrightarrow{H_2O} 2NH_4Cr(SO_4)_2 \cdot 12H_2O + 3H_2 \quad (11)$$

To study the effect of ammonium sulfate addition, seven experiments were designed (see Table 4). *Note*: The experiments with $R_{AS}$ = −100% corresponded to no addition of $(NH_4)_2SO_4$. The experiments were performed for the following quantities of $(NH_4)_2SO_4$ addition: 0% (stoichiometric amount), 80.4% and 170.6% excess of ammonium sulfate. The operational conditions were determined as follows: process time = 2 h; temperature – 150 °C and 60 wt% $H_2SO_4$ solution; temperature – 170 °C and 75 wt% $H_2SO_4$ solution.

## 3. Results and discussion

The results obtained during this study are summarized in two parts: First part shows the response surface methodology for the chosen independent variables (temperature ($T$), $H_2SO_4$ mass concentration on leaching solution ($C$) and time of reaction ($t$)), models validation and process optimization. Second part presents the effects of perchloric acid and ammonium sulfate additions on the reaction system.

### 3.1. Box–Behnken quadratic response surface

The experimental and simulated results obtained using Box–Behnken design are shown in Table 5.

The experimental variance was considered uniform with no-correlated experiments; its value was obtained on the basis of three replicates performed at the central point of experimental region (levels 0, 0, 0 of coded factors). The experimental confidential interval (98% significant level) calculated (normal test) was ±7.2% for Fe conversion and ±4.9% for Cr conversion.

Initially, the general solution of linear parameter model (including 10 parameters, see Eq. (1)) was applied and the adequacy of the model was tested by $F$-test (Eq. (7) see values in Table 6). Further, $t$-test has been applied (98% significant level) on model parameters to estimate their validity. The null hypothesis considered the parameters' value equal to zero. The variance associated with each parameter was determined by calculation of parameter covariance matrix and its main diagonal. Hence, only parameters significantly different from zero were reconsidered. The adequacy

**Table 5**
Experimental and simulated results in Box–Benhken design.

| Run | $t$ (h)[a] | $T$ (°C)[a] | $C$ (%)[a] | Experimental[b] | | Fitted[c] | |
|---|---|---|---|---|---|---|---|
| | | | | $X_{Fe}$ (%) | $X_{Cr}$ (%) | $X_{Fe}$ (%) | $X_{Cr}$ (%) |
| 1 | 1 (−1) | 130 (−1) | 75 (0) | 74.2 | 71.4 | 77.2 ± 9.6 | 72.5 ± 8.1 |
| 2 | 3 (+1) | 130 (−1) | 75 (0) | 75.4 | 68.2 | 77.2 ± 9.6 | 76.8 ± 8.1 |
| 3 | 3 (+1) | 170 (+1) | 75 (0) | 73.7 | 90.0 | 77.2 ± 9.6 | 88.9 ± 8.1 |
| 4 | 1 (−1) | 170 (+1) | 75 (0) | 78.6 | 69.0 | 77.2 ± 9.6 | 60.4 ± 8.1 |
| 5 | 1 (−1) | 130 (0) | 60 (−1) | 63.9 | 53.8 | 69.3 ± 11.0 | 56.5 ± 8.1 |
| 6 | 3 (+1) | 130 (0) | 60 (−1) | 82.3 | 98.9 | 86.6 ± 11.0 | 95.2 ± 8.1 |
| 7 | 3 (+1) | 170 (0) | 90 (+1) | 59.1 | 75.5 | 57.1 ± 11.0 | 72.8 ± 8.1 |
| 8 | 1 (−1) | 170 (0) | 90 (+1) | 75.4 | 74.1 | 74.4 ± 11.0 | 78.9 ± 8.1 |
| 9 | 2 (0) | 110 (−1) | 60 (−1) | 72.3 | 69.2 | 64.6 ± 11.0 | 66.3 ± 7.8 |
| 10 | 2 (0) | 150 (+1) | 60 (−1) | 79.9 | 74.2 | 77.9 ± 11.0 | 84.0 ± 7.8 |
| 11 | 2 (0) | 190 (+1) | 90 (+1) | 48.1 | 63.3 | 52.4 ± 11.0 | 66.3 ± 7.8 |
| 12 | 2 (0) | 150 (−1) | 90 (+1) | 67.0 | 93.7 | 65.7 ± 11.0 | 84.0 ± 7.8 |
| 13 | 2 (0) | 150 (0) | 75 (0) | 83.2 | 87.3 | | |
| 14 | 2 (0) | 150 (0) | 75 (0) | 85.8 | 89.9 | 83.9 ± 9.7 | 89.6 ± 7.3 |
| 15 | 2 (0) | 150 (0) | 75 (0) | 89.4 | 91.5 | | |

[a] Numbers in parentheses indicate the correspondent level of independent variables.
[b] Confidence interval of ±4.9 for Cr and ±7.2 for Fe (normal test).
[c] Confidence interval calculated by $t$-test.

**Table 6**
ANOVA table: $F$-test for the studied models.

| Groups | | Variability between groups | | Variability within group "B" | | $F$-test values | | Model prediction quality | |
|---|---|---|---|---|---|---|---|---|---|
| A[a] | B[a] | Sum of squares | Degrees of freedom | Sum of squares | Degrees of freedom | $F_0$ | $F_{critic}$[b] | $R^2$ | $R^2_{adj}$ |
| | | | | Iron | | | | | |
| 10 P | Exp | 129 | 5 | 19 | 2 | 2.7 | 49.3 | 0.921 | 0.780 |
| 6 P | Exp | 197 | 9 | 19 | 2 | 2.3 | 49.4 | 0.880 | 0.813 |
| 6 P | 10P | 68 | 4 | 129 | 5 | 0.7 | 8.2 | – | – |
| | | | | Chromium | | | | | |
| 10 P | Exp | 410 | 5 | 9.0 | 2 | 18 | 49 | 0.830 | 0.525 |
| 8 P | Exp | 426 | 7 | 9.0 | 2 | 14 | 49 | 0.824 | 0.648 |
| 8 P | 10 P | 16 | 2 | 410 | 5 | 0.09 | 9.45 | – | – |

[a] Exp: experimental; 10 P: model with 10 parameters; 8 P: model with 8 parameters; 6 P: model with 6 parameters.
[b] Critical values of $F$-test with 98% level of significance.

**Table 7**
Simplified quadratic models with evaluated values of significant parameters for Cr and Fe.

| Parameter | $i$ = Cr | $i$ = Fe |
|---|---|---|
| | Value ± Var[a] | Value ± Var[a] |
| $b^i_0$ | 89.6 ± 3.7 | 83.9 ± 4.2 |
| $b^i_1$ | – | −6.10 ± 3.11 |
| $b^i_2$ | – | – |
| $b^i_3$ | 8.18 ± 2.25 | – |
| $b^i_{12}$ | −8.85 ± 3.18 | −6.63 ± 4.39 |
| $b^i_{13}$ | −11.2 ± 3.2 | −8.68 ± 4.39 |
| $b^i_{23}$ | 6.05 ± 3.18 | – |
| $b^i_{11}$ | −6.63 ± 3.31 | −12.0 ± 4.6 |
| $b^i_{22}$ | −7.83 ± 3.31 | −6.72 ± 4.56 |
| $b^i_{33}$ | −7.08 ± 3.31 | – |
| $R^2$ | 0.824 | 0.880 |
| $R^2_{adj}$ | 0.648 | 0.813 |

[a] Confidence interval calculated by $t$-test.

of the obtained new model was tested by applying $F$-test (see Table 6 and Eq. (7)). In addition, the $F$-test was applied for comparison of the initial and simplified models (see Table 6, where Eq. (8) was used). In Table 6, the predictive quality of models represented by $R^2$ (Eq. (5)) and $R^2_{adjusted}$ (Eq. (6)) values is shown, as well.

Analyzing the results presented in Table 6, one can conclude that models with 8 and 6 parameters were adequate for prediction of chromium and iron conversions, respectively. The parameters significantly different from zero are shown in Table 7. The confidence interval for each parameter has been calculated using $t$-test (98% significant level) as mentioned above.

The confidence interval of model parameters, shown in Table 5, was based on $t$-test with variance obtained from the main diagonal of error-predicted covariance matrix.

Analyzing the results obtained from chromium conversion model (see Table 7), the linear effect between the parameters associated with factors $C$ (concentration of sulfuric acid) and $T$ (temperature) was insignificant. However, the interaction and the quadratic effects were significant. The obtained response surface results for Cr conversion are shown in Fig. 1.

Table 7 also contains the significant parameter values of iron conversion model. Parameters associated with linear effect of $T$ (temperature), process $t$ (time), interaction effect of this factors, and quadratic effect of factor "$t$" were insignificant. Fig. 2 shows the response surfaces obtained for Fe conversions.

Figs. 3 and 4 present the results obtained from chromium and iron conversion models, respectively, when two-dimensional graph is used. In Fig. 3(a) one can observe that an increase of temperature and the process time reflects in a significant increase of the Cr conversion (applying 60 wt% of sulfuric acid concentration) until maximum conversion. Fig. 4(a) presents the same tendency for Fe conversion when applying same concentration of sulfuric acid. For sulfuric acid concentration of 75 wt%, (see Fig. 3(b)), an increase of conversion can be observed for the following conditions—temperature between 140 and 160 °C, and process time between 1 and 3 h. For process duration above 3 h conversion level decreases. The iron conversion model presents does not depend on process time between 1 and 3 h for 75 wt% $H_2SO_4$ (see Fig. 4(b)); the temperature increase up to 150 °C causes a slight increase of Fe conversion, and above this value the conversion return to its previous levels. For $C$ = 90 wt% $H_2SO_4$ (see Fig. 3(c)), the time increase as well as temperature increase above 170 °C tends to decrease the chromium conversion. The prediction of iron conversion model for 90 wt% $H_2SO_4$ concentration and all applied process times (see Fig. 4(c)) shows that for temperature values above 170 °C a reduction of Cr conversion is observed.

The phenomenon associated with decreasing of the conversions when the control variables (process time, temperature and $H_2SO_4$ concentration) were above their optimal values can be explained by a formation of low stoichiometric hydrated sulfates (anhydrous sulfates), which were also reported by Vardar et al. [29]. In addition, when higher sulfuric acid concentration was applied, an effect of decreasing of the acid activity may occur, as reported by Robertson and Dunford [35].

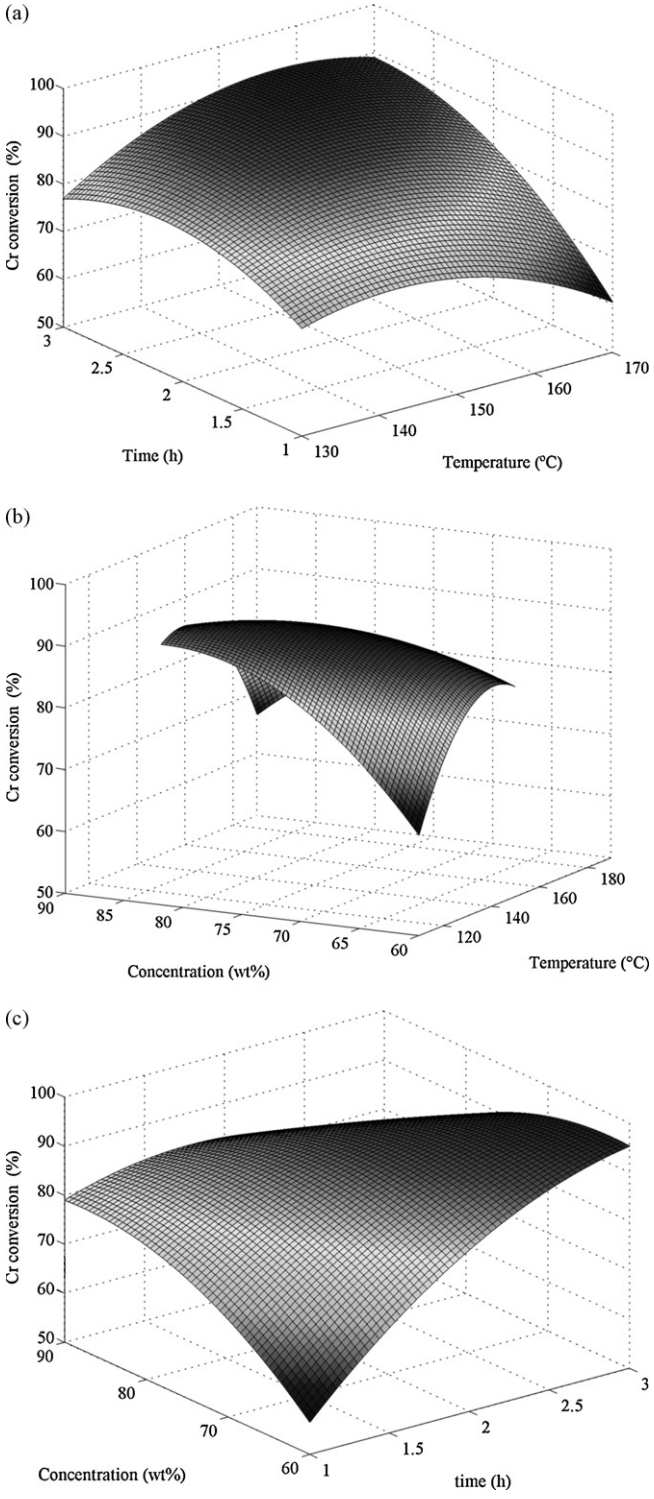


**Fig. 1.** Chromium conversion response surfaces as a function of: (a) process time and temperature, for 75 wt% $H_2SO_4$ concentration; (b) $H_2SO_4$ concentration and temperature for process time = 2h; (c) $H_2SO_4$ concentration and process time, for temperature at level zero of coded variable ($T$ = 50 + 1.33 C).

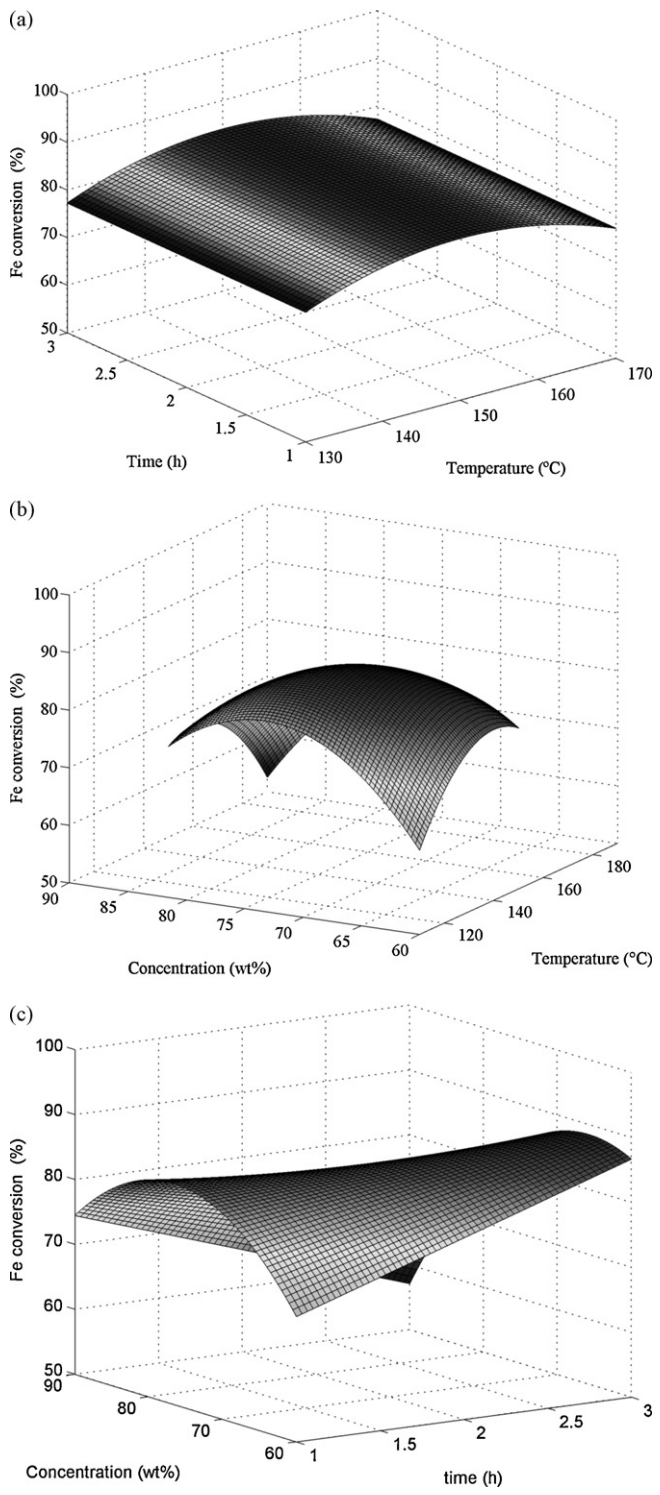


**Fig. 2.** Iron conversion response surfaces as a function of: (a) process time and temperature, for 75 wt% $H_2SO_4$ concentration; (b) $H_2SO_4$ concentration and temperature, and process time = 2 h; (c) $H_2SO_4$ concentration and process time, for the temperature at level zero of coded variable ($T = 50 + 1.33\,C$).

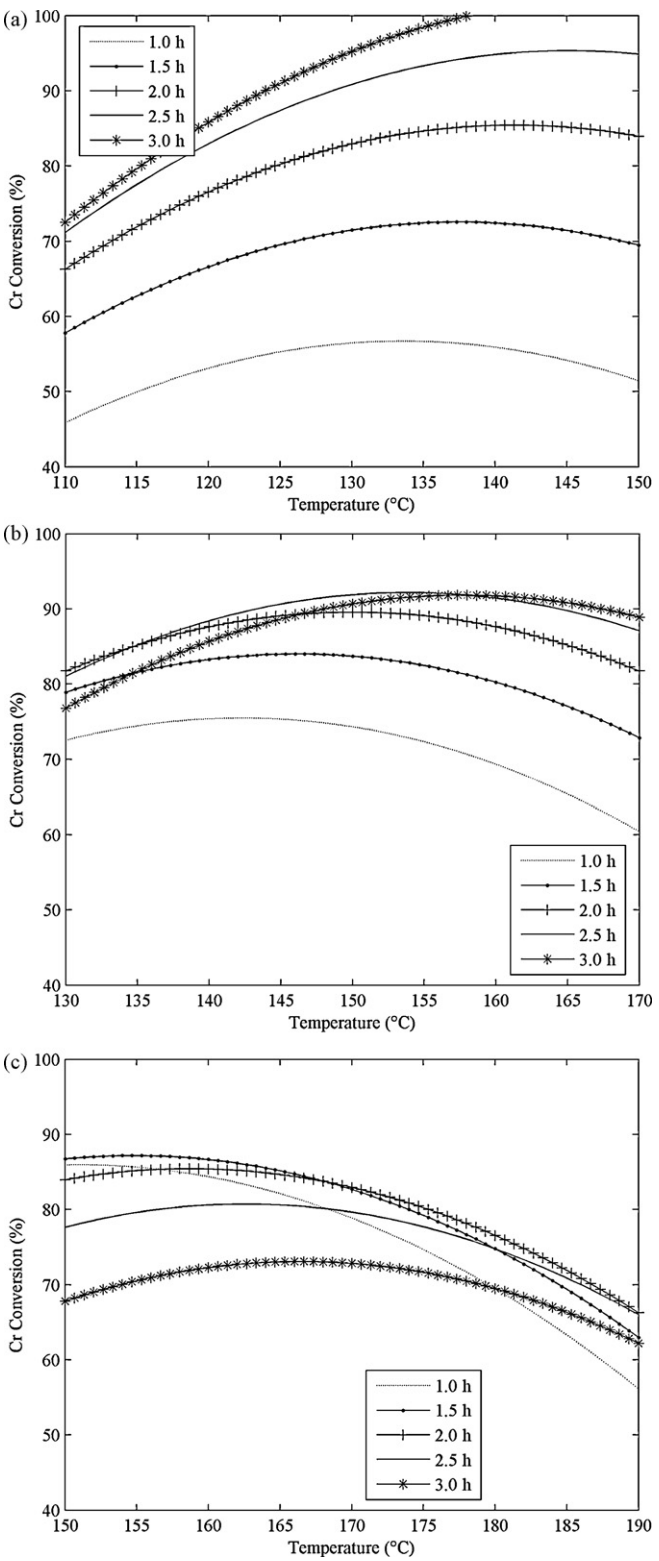


**Fig. 3.** Chromium conversion vs. temperature for process times of 1.0, 1.5, 2.0, 2.5 and 3.0 h and for different sulfuric acid concentrations: (a) 60 wt%; (b) 75 wt%; (c) 90 wt%.

For maximization of Cr and Fe conversions, a scalar optimization method presented by Eq. (10) was utilized. Table 8 shows the optimal parameters' values ($C$, $T$ and $t$) in respect to the obtained conversions and objective function value as a function of "chromium weight". The operational parameters did not vary significantly ($C = 60.0$–$64.3$ wt%, $T = 143$–$149\,^{\circ}C$, $t = 3.00$ h) as a function of "chromium weight" variation in the range from 0 to 1. The conversions at maximum points were about 98.6–100% for Cr and 86.9–89.1% for Fe. The obtained results suggested that the Cr is leached in a higher proportion than Fe. It must be noticed that the anhydrous sulfates formation effect was out of consideration.

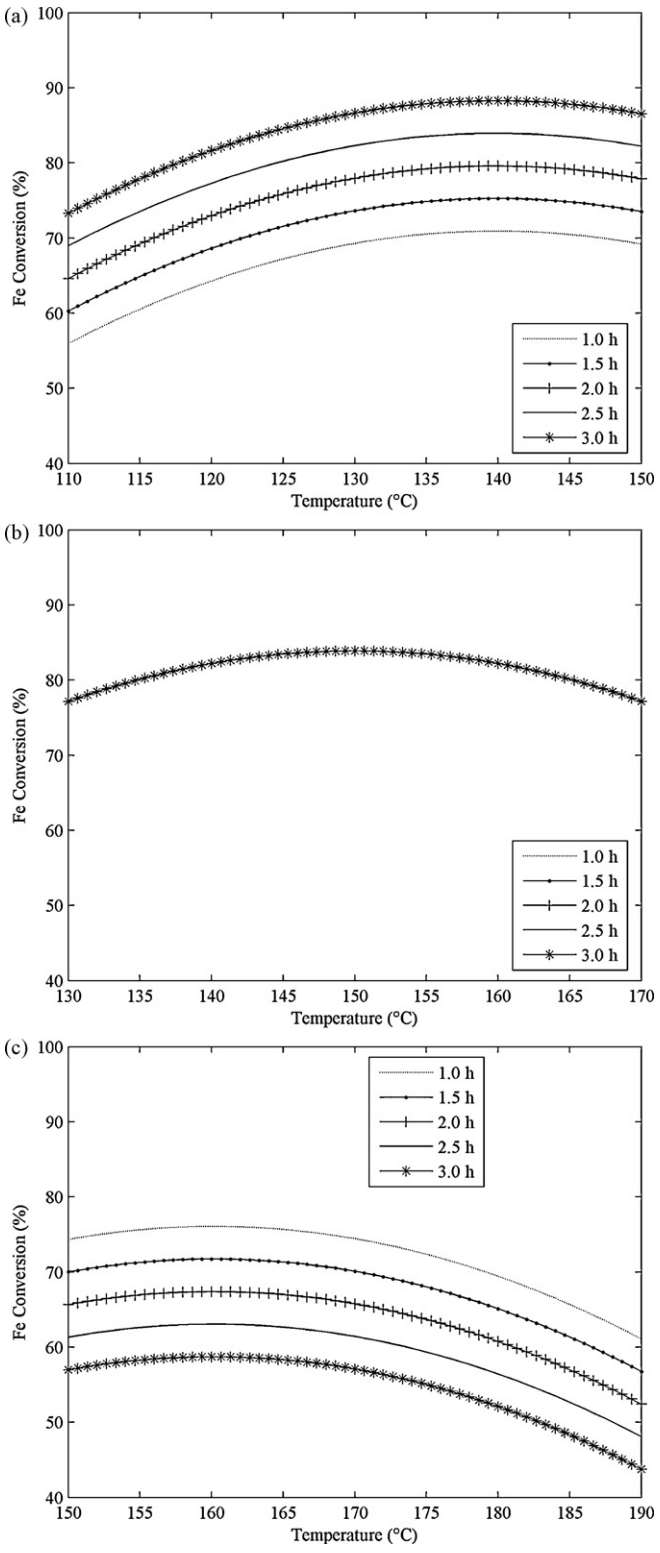


**Fig. 4.** Iron conversion vs. temperature for process times of 1.0, 1.5, 2.0, 2.5 and 3.0 h and for different sulfuric acid concentrations: (a) 60 wt%; (b) 75 wt%; (c) 90 wt%.

### 3.2. Effect of perchloric acid and ammonium sulfate addition

Independent runs of experiments were designed in order to study the effect of perchloric acid ($HClO_4$) and ammonium sulfate ($(NH_4)_2SO_4$) additions. The $HClO_4$ addition increased the acid power of reaction solution, and as a result the links in the Fe–Cr–HC alloy were broken. On the other hand, the utilization of $(NH_4)_2SO_4$ influenced the behavior of the reaction system by decreasing the quantities of anhydrous sulfates which resulted in formation of ammonium alum with iron(III) or chromium(III) compounds.

**Table 8**
Optimization results for $C$, $T$ and $t$ factors connected with Cr and Fe conversion, respectively and the objective function value vs. "chromium weight" values.

| $w_{Cr}$ | $C$ (wt%) | $T$ (°C) | $t$ (h) | $X_{Cr}$ (%) | $X_{Fe}$ (%) | $F_{obj}$ |
|---|---|---|---|---|---|---|
| 0.0 | 64.3 | 143 | 3.00 | 98.6 | 89.1 | 89.1 |
| 0.1 | 63.7 | 143 | 3.00 | 99.3 | 89.1 | 90.1 |
| 0.2 | 63.0 | 144 | 3.00 | 100.0 | 89.0 | 91.2 |
| 0.3 | 62.1 | 144 | 3.00 | 100.6 | 88.8 | 92.3 |
| 0.4 | 61.1 | 145 | 3.00 | 101.3 | 88.4 | 93.6 |
| 0.5 | 60.0 | 145 | 3.00 | 102.0 | 87.9 | 94.9 |
| 0.6 | 60.0 | 146 | 3.00 | 102.1 | 87.7 | 96.3 |
| 0.7 | 60.0 | 147 | 3.00 | 102.2 | 87.5 | 97.8 |
| 0.8 | 60.0 | 147 | 3.00 | 102.3 | 87.3 | 99.3 |
| 0.9 | 60.0 | 148 | 3.00 | 102.3 | 87.1 | 100.8 |
| 1.0 | 60.0 | 149 | 3.00 | 102.3 | 86.9 | 102.3 |

The operational conditions of perchloric acid addition study were as follows: process time = 2 h and 75 wt% concentration of sulfuric acid solution. The process temperatures were determined as 140 and 170 °C. The $R_{PA}$ independent variable was changed by increments of 0.25 in the range from zero to 0.5 ml of 70% $HClO_4$/g of Fe–Cr–HC. The obtained results are shown in Fig. 5.

Fig. 5 shows a decrease of soluble chromium and iron conversions, most probably due to a formation of chromium and iron anhydrous sulfates (insoluble) in the presence of high oxidative power of perchloric acid. Such a formation of insoluble chromium compounds was also observed in the work of Vardar et al. [29] where similar system was studied.

The effect of the ammonium sulfate was studied through the variation of $R_{SA}$ (150 °C/60 wt% and 170 °C/75 wt% of $H_2SO_4$ solutions) independent variable during the 2 h process time. Control experiments with no addition of $(NH_4)_2SO_4$ (−100% excess) were performed, together with experiments involving different stoichiometric amounts of $(NH_4)_2SO_4$ in order to achieve 0%, 80.4% and 170.6% excess of chromium–ammonium alum. Fig. 6 shows the results from these experiments.

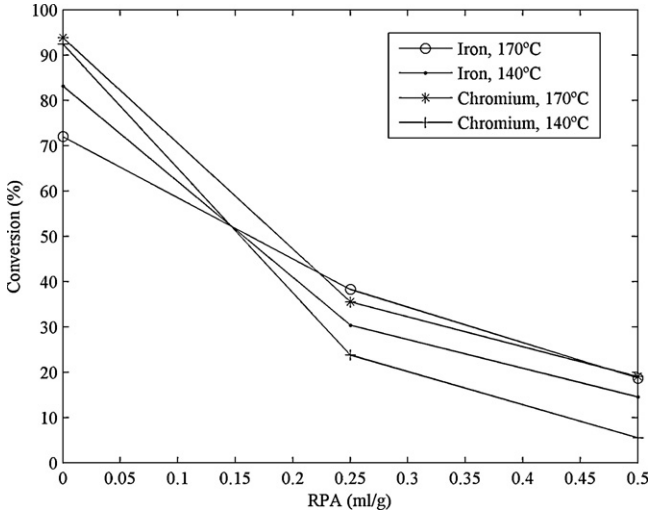


**Fig. 5.** Chromium and iron conversions as a function of perchloric acid addition for the given operational conditions: $t$ = 2 h, $C$ = 75 wt%, $T$ = 140 and 170 °C.

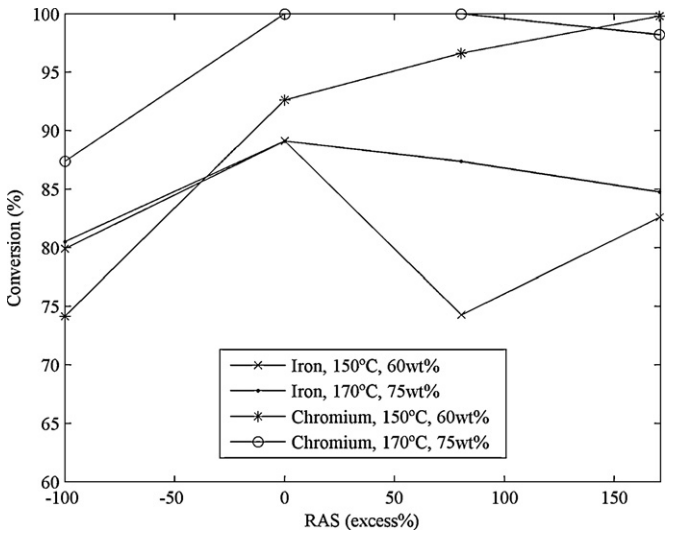


**Fig. 6.** Chromium and iron conversions vs. $(NH_4)_2SO_4$ addition for the given conditions: $t$ = 2 h. $T$ = 150 °C/$C$ = 60 wt% and $T$ = 170 °C/$C$ = 75 wt%.

Analysis of Fig. 6 showed that the addition of $(NH_4)_2SO_4$ contributed for the solubilization of chromium compounds. For the given conditions of 170 °C, 75 wt% $H_2SO_4$ solution, and addition of stoichiometric amount of $(NH_4)_2SO_4$ (0.665 g/g Fe–Cr–HC), the conversion of soluble chromium compounds was approximately 100%. In view of the confidence experimental interval for iron conversion (±7.2%), it was concluded that the presence of ammonium sulfate had no effect on the Fe conversion. Hence, the obtained results proved the hypothesis that the chromium no-conversion part included low stoichiometric hydrated sulfates.

## 4. Conclusions

This study proposed an effective method for production of soluble iron and chromium sulfate complex (tanning agent), which can be obtained from high carbon ferrochromium alloy. The non-equilibrium chemical reaction between Fe–Cr–HC and sulfuric acid was studied by applying the Box–Behnken experimental design for the following chosen factors: temperature, sulfuric acid concentration, and process time. The quadratic response surface methodology helped to find the optimal conditions for maximization of iron and chromium conversions: $C$ = 60.0–64.3 wt%, $T$ = 143–149 °C, $t$ = 3.00 h. For the given range of operational parameters, the maximum Cr and Fe conversions were 98.6–100% and 86.9–89.1%, respectively. The obtained results suggested that the Cr is leached in a higher proportion than Fe. The addition of perchloric acid into the reaction system decreased the quantity of soluble chromium and iron compounds because of the anhydrous sulfates formation. An increase of chromium conversion was observed during the experiments with ammonium sulfate addition most probably due to a formation of soluble chromium–ammonium alum.

## Acknowledgements

The authors are very grateful to CAPES and CNPq for the financial support and to Alexander D. Kroumov, Ph.D. for the review and helpful comments on the manuscript.

## References

[1] S. Langard, 100 years of chromium and cancer—a review of epidemiological evidence and selected case-reports, Am. J. Ind. Med. 17 (1990) 189–215.
[2] T.-C. Tsou, R.-J. Lin, J.-L. Yang, Mutational spectrum induced by chromium(III) in shuttle vectors replicated in human cells: relationship to Cr(III)–DNA interactions, Chem. Res. Toxicol. 10 (1997) 962–970.
[3] L.J. Blankenship, F.C.R. Manning, J.M. Orenstein, S.R. Patierno, Apoptosis is the mode of cell-death caused by carcinogenic chromium, Toxicol. Appl. Pharmacol. 126 (1994) 75–83.
[4] S. Deflora, M. Bagnasco, D. Serra, P. Zanacchi, Genotoxicity of chromium compounds—a review, Mut. Res. 238 (1990) 99–172.
[5] Z. Zaroual, H. Chaair, A.H. Essadki, K. El Ass, M. Azzi, Optimizing the removal of trivalent chromium by electrocoagulation using experimental design, Chem. Eng. J. 148 (2009) 488–495.
[6] F.R. Espinoza-Quiñones, M.M.T. Fornari, A.N. Módenes, S.M. Palácio, F.G. da Silva Jr., N. Szymanski, A.D. Kroumov, D.E.G. Trigueros, Pollutant removal from tannery effluent by electrocoagulation, Chem. Eng. J. 151 (2009) 59–65.
[7] N.N. Fathima, J.R. Rao, B.U. Nair, Chromium(VI) formation: thermal studies on chrome salt and chrome tanned hide powder, J. Am. Leather Chem. Assoc. 96 (2001) 444–450.
[8] R. Milacic, J. Stupar, Fractionation and oxidation of chromium in tannery waste- and sewage sludge-amended soils, Environ. Sci. Technol. 29 (1995) 506–514.
[9] K.J. Sreeram, T. Ramasami, Sustaining tanning process through conservation, recovery and better utilization of chromium, Resour. Conserv. Recycl. 38 (2003) 185–212.
[10] S.E. Kentish, G.W. Stevens, Innovations in separations technology for the recycling and re-use of liquid waste streams, Chem. Eng. J. 84 (2001) 149–159.
[11] M. Godinho, N.R. Marcilio, A.C. Faria Vilela, L. Masotti, C.B. Martins, Gasification and combustion of the footwear leather wastes, J. Am. Leather Chem. Assoc. 102 (2007) 182–190.
[12] M. Godinho, N.R. Marcilio, L. Masotti, C.B. Martins, D.E. Ritter, B.M. Wenzel, Formation of PCDD and PCDF in the thermal treatment of footwear leather wastes, J. Hazard. Mater. 167 (2009) 1100–1105.
[13] A. Dettmer, K.G.P. Nunes, M. Gutterres, N.R. Marcílio, Obtaining sodium chromate from ash produced by thermal treatment of leather wastes, Chem. Eng. J. 160 (1) (2010) 8–12, doi:10.1016/j.cej.2010.02.018.
[14] B.M. Wenzel, N.R. Marcilio, J.L. Klug, N.C. Heck, M. Godinho, Production of high carbon ferrochromium alloy from footwear leather waste ash through a carbothermic reduction, J. Hazard. Mater., under review.
[15] A. Dettmer, K.G.P. Nunes, M. Gutterres, N.R. Marcílio, Production of basic chromium sulfate by using recovered chromium from ashes of thermally treated leather, J. Hazard. Mater. 176 (2010) 710–714.
[16] A. Reife, E. Weber, H.S. Freeman, Iron: producing more than rust in our environment, Chemtech 27 (1997) 17–25.
[17] C. Gaidau, F. Platon, N. Badea, Investigation into iron tannage, J. Soc. Leather Technol. Chem. 82 (1998) 143–146.
[18] J.R. Rao, P. Thanikaivelan, J. Malathi, R. Rajaram, B.U. Nair, Development of natural colours in Cr–Fe tanned garment leathers, J. Soc. Leather Technol. Chem. 86 (2002) 106–111.
[19] R. Rao, Thanikaivelan, P. Thanikaivelan, B Nair, An eco-friendly option for less-chrome and dye-free leather processing: in situ generation of natural colours in leathers tanned with Cr–Fe complex, Clean Techn. Environ. Policy 4 (2002) 115–121.
[20] N. Bensalah, M.A.Q. Alfaro, C.A. Martínez-Huitle, Electrochemical treatment of synthetic wastewaters containing Alphazurine A dye, Chem. Eng. J. 149 (2009) 348–352.
[21] N.N. Fathima, M. Chandrabose, R. Aravindhan, J.R. Rao, B.U. Nair, Iron–phosphonium combination tanning: towards a win-win approach, J. Am. Leather Chem. Assoc. 100 (2005) 273–281.
[22] N.N. Fathima, M.C. Bose, J.R. Rao, B.U. Nair, Stabilization of type I collagen against collagenases (type I) and thermal degradation using iron complex, J. Inorg. Biochem. 100 (2006) 1774–1780.
[23] E.L. Tavani, N.A. Lacour, Making of iron(III) tanning salts from a waste of the titanium recovery by the sulphate process, Mater. Chem. Phys. 72 (2001) 380–386.
[24] J.R. Rao, K.J. Sreeram, P. Thanikaivelan, B.U. Nair, T. Ramasami, in: Indian Patent Office (Ed.), A process for the preparation of a novel chromium–iron complex for use in leather industry, Intellectual Property Office, Application Number 446/DEL/99, India, 1999, pp. 30.
[25] V. Suresh, M. Kanthimathi, P. Thanikaivelan, J. Raghava Rao, B. Unni Nair, An improved product-process for cleaner chrome tanning in leather processing, J. Cleaner Prod. 9 (2001) 483–491.
[26] V. Plavan, V. Valeika, O. Kovtunenko, J. Sirvaityte, Thps pretreatment before tanning (chrome or non-chrome), J. Soc. Leather Technol. Chem. 93 (2009) 186–192.
[27] S. Ray, J.A. Lalman, N. Biswas, Using the Box–Benkhen technique to statistically model phenol photocatalytic degradation by titanium dioxide nanoparticles, Chem. Eng. J. 150 (2009) 15–24.
[28] R. Kumar, R. Singh, N. Kumar, K. Bishnoi, N.R. Bishnoi, Response surface methodology approach for optimization of biosorption process for removal of Cr (VI), Ni (II) and Zn (II) ions by immobilized bacterial biomass sp. Bacillus brevis, Chem. Eng. J. 146 (2009) 401–407.
[29] E. Vardar, R.H. Eric, F.K. Letowski, Acid leaching of chromite, Miner. Eng. 7 (1994) 605–617.
[30] CETSNRC, High-Purity Chromium Metal: Supply Issues for Gas-Turbine Superalloys, in: C.o.H.-P.E.C.M. NMB-480 (Ed.), National Academy Press, Washington, D.C., 1995.
[31] A.M. Dean, D.T. Voss, Design and Analysis of Experiments, 1st ed., Springer-Verlag, New York, 1999.

[32] T.F. Coleman, Y.Y. Li, An interior trust region approach for nonlinear minimization subject to bounds, SIAM J. Optim. 6 (1996) 418–445.
[33] K. Yates, H. Wai, A redetermination and extension of the homicron scale of acidity in aqueous perchloric acid, J. Am. Chem. Soc. 86 (1964) 5408–5413.
[34] K. Winnacker, E. Weingartner, Tecnología Química Tomo II—Química Industrial Inorgânica, Editora Gustavo Gili S.A, Barcelona, 1953.
[35] E.B. Robertson, H.B. Dunford, The state of the proton in aqueous sulfuric acid, J. Am. Chem. Soc. 86 (1964) 5080–5089.